

Sol–gel derived bioglass as a coating material for porous alumina scaffolds

Jianli Liu, Xigeng Miao*

School of Materials Engineering, Nanyang Technological University, Nanyang Avenue, Singapore 639798, Singapore

Received 12 November 2003; received in revised form 11 December 2003; accepted 22 December 2003

Available online 6 May 2004

Abstract

Bioglasses are important bioactive materials and have been used for the repair and reconstruction of diseased bone tissues, as they exhibit direct bonding with human bone tissues. However, bioglasses have low mechanical properties and thus are usually used as coatings on strong substrates. A sol–gel method was used in this study to produce the 58S bioglass powder with the composition of 58 mol% SiO_2 –38 mol% CaO –4 mol% P_2O_5 . The bioglass powder was then pressed into discs and sintered at 500, 800, 1000, and 1200 °C, respectively. The apparent density and the Vicker's hardness of the sintered bioglass were tested using a densometer and a Vicker's hardness tester. The thermal properties of the bioglass were also studied using differential scanning calorimetry (DSC) and dilatometry. The crystallization of the bioglass was examined using X-ray diffraction (XRD) and scanning electron microscopy (SEM). The sintered bioglass discs were then immersed in the simulated body fluid (SBF) solution. The bioglass surface after the immersion was examined using field emission scanning electron microscopy (FE-SEM). The formation of apatite layer was confirmed using Fourier transform infrared spectroscopy (FTIR). The apparent density and the hardness of the bioglass reached 3.12 g/cm³ at 1000 °C and 1.05 GPa at 1200 °C, respectively. The formation of hydroxyl-carbonate apatite layer confirmed the bioactivity of the bioglass. It was also found that at sintering temperatures above 800 °C, crystalline phase CaSiO_3 was formed. With the formation of CaSiO_3 , the bioactivity of the bioglass started to decrease.

© 2004 Elsevier Ltd and Techna Group S.r.l. All rights reserved.

Keywords: Sol–gel; Bioglass; Crystallinity; Bioactivity; Coating

1. Introduction

Over the last decade or so, several kinds of bioceramics have been studied for treating damaged and diseased bones [1,2]. Namely, they are bioinert ceramics (e.g., alumina and zirconia), bioactive ceramics (e.g., bioglasses and hydroxyapatite) and biodegradable ceramics (e.g., tri-calcium phosphate and bone cement). Among these bioceramics, bioglass and glass-ceramics have attracted more and more attentions. As a kind of bioactive ceramics, the primary characteristic of bioglasses is their rapid rate of surface reaction, which leads to direct attachment to bone by a chemical bond [3]. The excellent bioactivity but low mechanical properties requires the bioglass to be used as coating for surface modification and bioactive phase in composites [4–6]. As a glass phase, bioglass also has relatively low softening temperature. Therefore, bioglass can be used as sintering aid to bond the

ceramic particles and fill the micropores during the sintering process [4,5]. More importantly, one advantage of bioactive glasses over other bioactive ceramics is the possibility of controlling a range of chemical properties and the rate of bonding to tissues. It is also possible to design glasses with properties specific to particular clinical applications [7].

A few methods have been developed to prepare the bioglasses. Melting method is the traditional one for glass preparation [8,9]. It is simple and suitable for massive production. However, during the high temperature stage, the volatile component P_2O_5 tends to escape. In recent years, sol–gel method has attracted many studies [10]. The sol–gel process has the advantage of low reaction temperature. Compared with the melting method, the sol–gel derived glass powder has homogenous composition in particles. A group of sol–gel derived bioglasses in the system of SiO_2 – CaO – P_2O_5 has been widely studied, such as 55S, 58S, 60S, etc. Their excellent bioactivity offers great potential for hard tissue surgery [10]. In the present paper, 58S sol–gel derived bioglass was chosen and the properties of

* Corresponding author. Tel.: +65-67904260; fax: +65-67909081.
E-mail address: asxgmiao@ntu.edu.sg (X. Miao).

58S bioglass as a coating material were studied. More importantly, the influence of the crystallization of the bioglass on the mechanical properties and the bioactivity were also studied.

2. Experimental procedure

Sol-gel derived 58S bioglass, with the composition of 58 mol% SiO_2 –38 mol% CaO –4 mol% P_2O_5 was used in the study. The glass was prepared by hydrolysis and polycondensation of tetraethyl orthosilicate (TEOS), triethyl phosphate (TEP) and $\text{Ca}(\text{NO}_3)_2 \cdot 4\text{H}_2\text{O}$. Solution HCl (1N) was used to catalyze the TEOS and TEP hydrolysis, with a molar ratio of $(\text{HCl} + \text{H}_2\text{O})/(\text{TEOS} + \text{TEP}) = 8$. Each reactant was consecutively added under continuous stirring. The solution was then aged in an oven at 60°C for 48 h. The dried gel was then calcined at 700°C for 2 h, followed by 4 h ball milling to obtain the glass powder. To study the thermal properties of 58S bioglass, differential scanning calorimetry (DSC) (Thermal Analysis DSC 404C) measurement was carried out on the glass powder sample up to 1000°C at heating rate of $5^\circ\text{C}/\text{min}$. Thermal expansion measurement was carried out using a dilatometer (Unitherm, Anter Corp.). The sample for the dilatometry was produced via uniaxially die-pressing of the bioglass powder at 250 MPa, followed by sintering at 1200°C for 1 h.

The samples for other studies were prepared by uniaxial pressing of the bioglass powder at 250 MPa in a steel die to produce disks of 13 mm in diameter and 3 mm in thickness. Disks were then fired at 500, 800, 1000, and 1200°C , respectively, using a heating rate of $5^\circ\text{C}/\text{min}$. The set temperature was kept for 2 h and then the furnace was naturally cooled down. The apparent density and the Vicker's hardness of the sintered bioglass disks were tested using a densometer and a Vicker's hardness tester. The crystallization of the bioglass was examined using X-ray diffraction (XRD) (Lab XRD-6000 Shimadzu). The morphologies of the crystals in bioglass samples were observed using scanning electron microscopy (SEM) (SEM JEOL-JSM 5410). The sintered bioglass discs were separately immersed into the simulated body fluid (SBF) solution for 1 h, 6 h, 24 h, 3 days, and 7 days. The bioglass surface after the immersion was observed using field emission scanning electron microscopy (FE-SEM) (FESEM, JSM 6340). The formation of the apatite layer was analyzed using Fourier transform infrared spectroscopy (FTIR) (Perkin-Elmer S2000 FTIR spectrometer).

The ultimate purpose of the study was to use 58S bioglass as a coating material. Therefore, 58S bioglass coating was applied on alumina substrate via a dip coating method. The alumina specimen was formed via slip casting, followed by sintering at 1550°C for 2 h. Then the alumina specimen was dipped into a 50 wt.% 58S bioglass suspension for 5 min. After drying and firing at 1200°C for 1 h, a bioglass coating was formed on the alumina specimen.

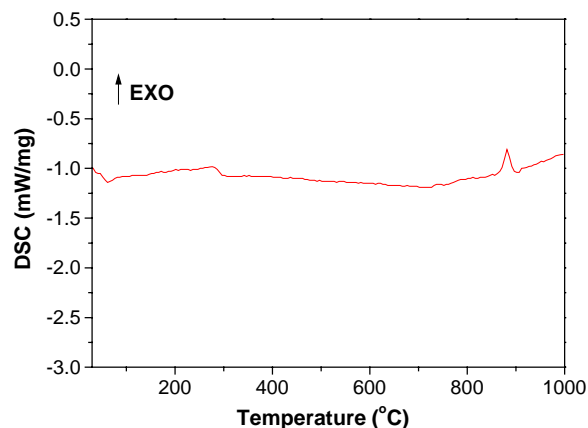


Fig. 1. DSC curve for the bioglass powder sample.

The coating was observed on a cross-section specimen using SEM.

3. Results and discussion

3.1. Thermal property analysis

Fig. 1 is the DSC graph of the 58S bioglass powder at the heating rate of $5^\circ\text{C}/\text{min}$. A weak endothermic peak can be noticed on the DSC curve at the range of 277 – 302°C , followed by an exothermic peak at the range of 848 – 903°C . The endothermic peak corresponded to the glass transition temperature of the bioglass, whereas the exothermic peak showed crystallization at the temperature of 848 – 903°C .

Fig. 2 shows the thermal expansion behavior of the 58S bioglass. It is clear that the sample expanded below 600°C . From the expansion curve, a coefficient of thermal expansion (CTE) of $0.73 \times 10^{-6}^\circ\text{C}^{-1}$ can be calculated. With the increase of temperature, the sample began to shrink, resulting from the softening of the 58S bioglass. Therefore, the softening temperature of the bioglass can be regarded as 600°C .

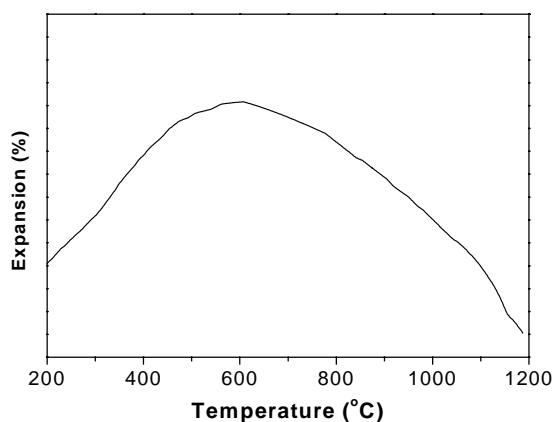


Fig. 2. Thermal expansion curve of 58S bioglass sample sintered at 1200°C for 1 h.

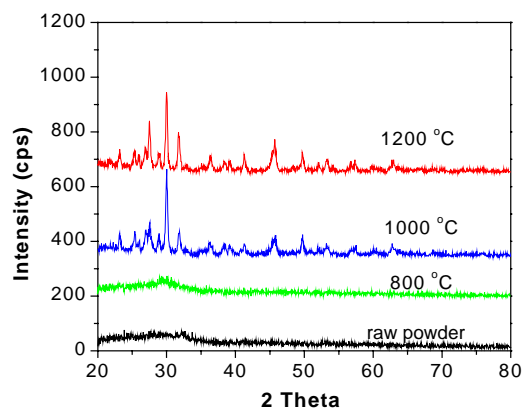


Fig. 3. XRD patterns of the 58S bioglass sintered at various temperatures.

3.2. Crystallization

The crystallization of the 58S bioglass is shown in Fig. 3. It can be seen that the starting 58S bioglass powder was amorphous, proving the sol–gel method could prepare pure glasses. As the temperature increased up to 800 °C, only a broad peak existed in the pattern, showing that the bioglass powder still kept the amorphous state. With further increase of the temperature, sharp peaks appeared at 1000 °C, indicating crystallization occurred in the 58S bioglass. The peaks matched the pattern of wollastonite CaSiO_3 (JCPDS #27-0088). The CaSiO_3 peaks became much sharper at 1200 °C, corresponding to further crystallization. The wollastonite CaSiO_3 crystals were also observed under SEM. Fig. 4 shows the wollastonite CaSiO_3 platelets existing in the bioglass sample sintered at 1200 °C. The wollastonite CaSiO_3 platelets had 3 μm in thickness.

3.3. Density and Vicker's hardness

Fig. 5 shows the apparent density of the 58S bioglass sintered at 500, 800, 1000 and 1200 °C. It can be seen that the

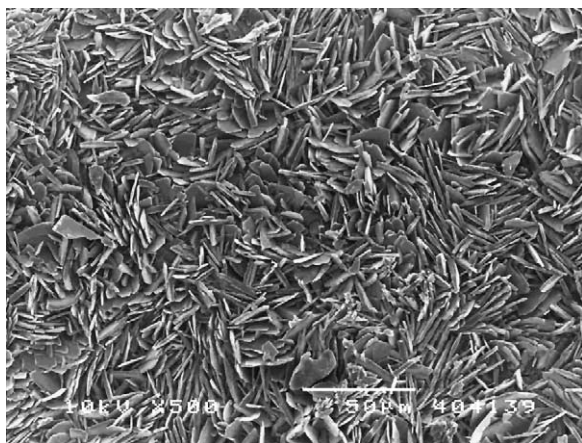


Fig. 4. SEM micrograph of CaSiO_3 crystals in glass sample sintered at 1200 °C.

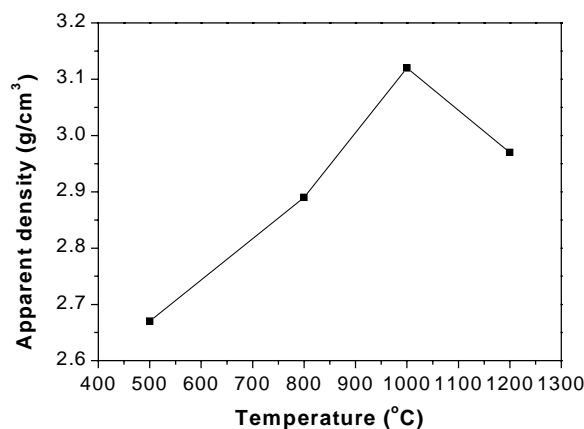


Fig. 5. Influence of sintering temperature on the density of the 58S bioglass samples.

sintered glass samples had relatively low density at low temperature due to the incomplete sintering of the samples. At 1000 °C the bioglass reached the maximum density. With the further increase of the temperature, the density decreased. It can be explained as the result of crystallization of the bioglass. During the crystallization, residual pores were left behind, resulting in the decrease of density. On the other hand, the Vicker's hardness of the 58S bioglass is shown in Fig. 6. The Vicker's hardness increased with the increase of sintering temperature. This was because the increase of the sintering temperature corresponded to the increased degree of crystallization, that is, more wollastonite CaSiO_3 existed in the glass matrix. It is known that the wollastonite phase has higher hardness than that of the amorphous glass. Therefore, after higher temperature sintering, more amount of wollastonite caused the increase of hardness of the 58S bioglass.

3.4. Bioactivity

To study the effect of crystallization on the bioactivity of 58S bioglass, samples sintered at 800 and 1000 °C were

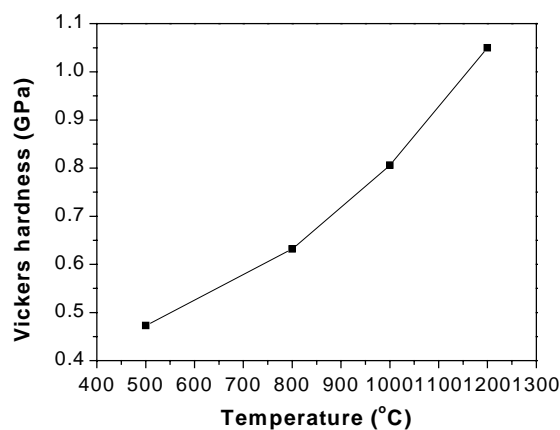
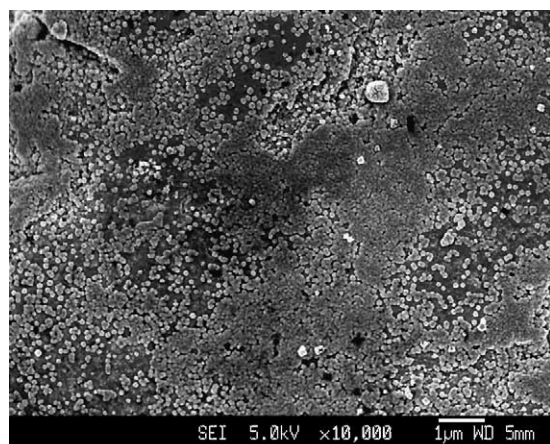
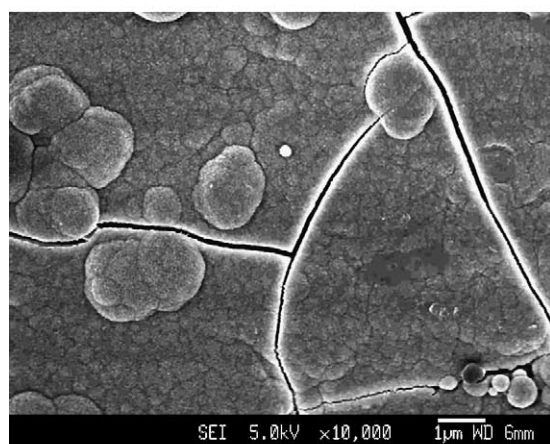


Fig. 6. Influence of sintering temperature on the Vicker's hardness of the 58S bioglass samples.



(a)



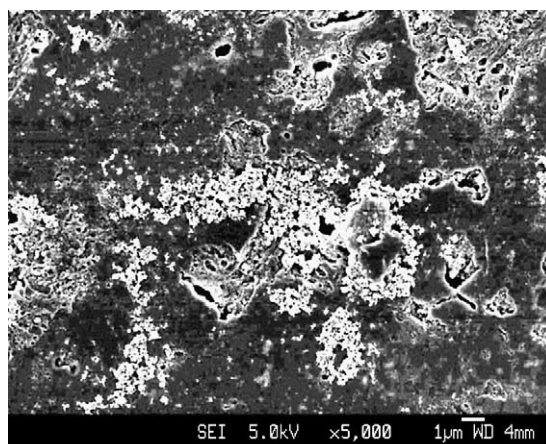
(b)

Fig. 7. SEM micrographs of the 58S bioglass sintered at 800 °C and after the immersion in SBF for 1 h (a), and 7 days (b).

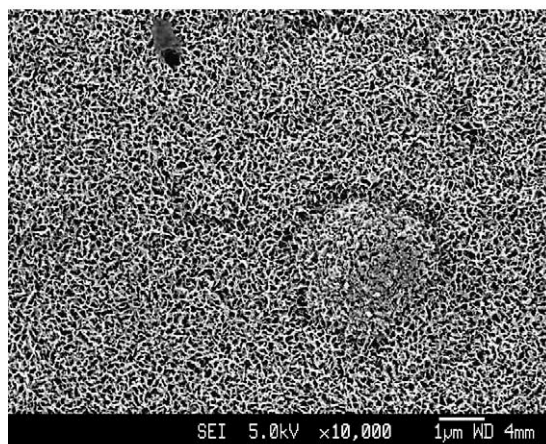
studied, corresponding to amorphous and crystallized samples. Figs. 7 and 8 show the micrographs of the 58S bioglass samples sintered at 800 and 1000 °C after immersion in the SBF for various times. The micrographs show the formation of apatite layer on the bioglass. From Fig. 7, it can be seen that the pure 58S bioglass exhibited excellent bioactivity. Apatite particles were observed on the surface of bioglass sample after 1 h immersion, as shown in Fig. 7a. The apatite crystals were round in shape and had particle sizes of 0.1 µm or so. After 7-day immersion, a fairly dense apatite layer was formed on the sample surface.

Fig. 8 shows the micrographs of the 58S bioglass sintered at 1000 °C after immersion in SBF for various times. These samples showed much lower bioactivity than those sintered at 800 °C. No apatite could be observed on the surface until after 24 h of immersion. After 7 days, a porous apatite layer was formed on the sample surface, in contrast to the dense apatite layer formed on the glass sample sintered at 800 °C. The decreased bioactivity of the 58S bioglass sample was due to the existing CaSiO_3 .

The apatite layers on the 58S bioglass samples were further analyzed using FTIR, as shown in Fig. 9. Well-defined



(a)



(b)

Fig. 8. SEM micrographs of the 58S bioglass sintered at 1000 °C and after the immersion in SBF for 24 h (a), and 7 days (b).

phosphate peak (P–O stretching peak) could be seen at 1000–1220 cm^{-1} , indicating the formation of amorphous $\text{CaO-P}_2\text{O}_5$ rich layer. Carbonate bands (C–O stretching peaks) were presented at 2350–2400 and 2500–2600 cm^{-1} , indicating the formation of carbonated apatite. In addition,

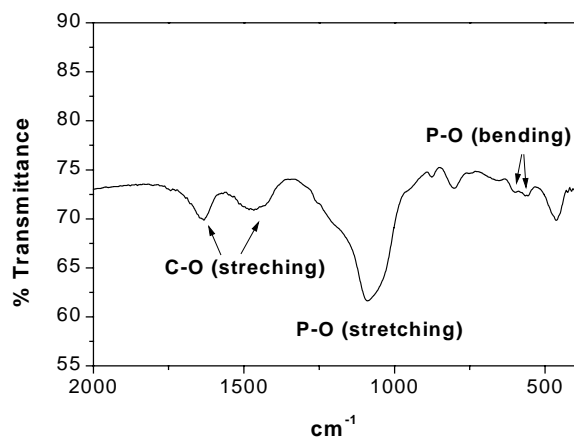


Fig. 9. FTIR curve of the apatite layer formed on the 58S bioglass sample.

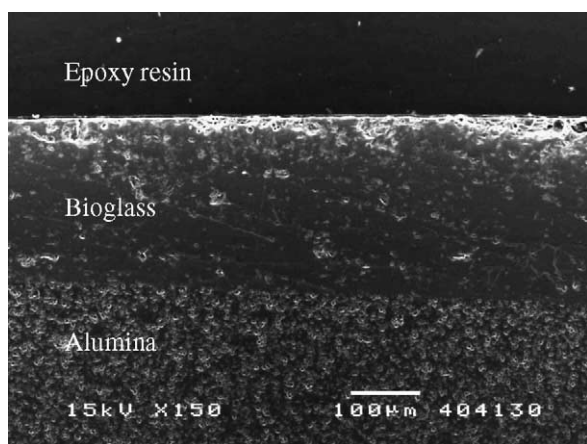


Fig. 10. SEM micrograph of the 58S bioglass coating on the alumina substrate.

P–O bending peak at $550\text{--}620\text{ cm}^{-1}$ was also observed in the FTIR spectra.

3.5. Bioglass coating on the alumina substrate

Fig. 10 shows the 58S bioglass coating on the alumina substrate. The 58S bioglass coating was $200\text{--}300\text{ }\mu\text{m}$ thick and was firmly attached to the alumina substrate. Generally speaking, to obtain a good coating, the CTE of the substrate and the coating materials must be matched. Otherwise, thermal stresses would exist between the substrate and coating to cause cracks or even peeling of the coating layer. In this study, the CTEs of 58S bioglass and alumina were measured as 0.73×10^{-6} and $9.47 \times 10^{-6}\text{ }^{\circ}\text{C}^{-1}$. Although the CTEs were quite different, the resultant thermal stresses could be relaxed due to the softening of the glass. In addition, due to the smaller CTE of the bioglass, the stresses in the coating could be compressive in nature. As a result, 58S bioglass could form a good bonding with the alumina substrate.

From the current study, it can be seen that the 58S bioglass coating would partially crystallized at $1200\text{ }^{\circ}\text{C}$. The crystallized 58S bioglass coating would form a porous apatite layer in vivo. The porous apatite layer would not only provide composition affinity with the bone tissue, but also induce the bone tissue ingrowth. Thus, the 58S bioglass coating not only could bond to the alumina substrate but also would bond to the bone tissue.

4. Conclusions

In this study, the sol–gel derived 58S bioglass was studied for use as a coating material. It was found that the

58S bioglass softened at $600\text{ }^{\circ}\text{C}$ and crystallized at the temperature range of $850\text{--}900\text{ }^{\circ}\text{C}$. The formation of the crystalline wollastonite phase limited the densification of the bioglass. However, the crystalline wollastonite phase increased the hardness of the 58S bioglass. The formation of the crystalline wollastonite phase also decreased the bioactivity of the 58S bioglass. A dense apatite layer was formed on the highly bioactive amorphous bioglass, whereas incomplete or porous apatite layer was formed on the bioglass subjected to crystallization. Finally, the 58S bioglass as a coating could attach to the alumina substrate.

Acknowledgements

The authors would like to acknowledge the financial support from the Nanyang Technological University (AcRF RG26/01).

References

- [1] L.L. Hench, J. Wilson, An Introduction to Bioceramics, World Scientific, Singapore, 1993, pp. 3–5.
- [2] L.L. Hench, Bioceramics: from concept to clinic, J. Am. Ceram. Soc. 74 (7) (1991) 1487.
- [3] L.L. Hench, Bioactive glass and glass-ceramics: a perspective, in: T. Yamamuro, L.L. Hench, J. Wilson (Eds.), Handbook of Bioactive Ceramics, CRC Press, Boca Raton, FL, 1990, p. 7.
- [4] M.A. Lopes, J.C. Knowles, J.D. Santos, Structural insights of glass-reinforced hydroxyapatite composites by Rietveld refinement, Biomaterials 21 (2000) 1905.
- [5] J.D. Santos, L.J. Jha, F.J. Monteiro, In vitro calcium phosphate formation on $\text{SiO}_2\text{--Na}_2\text{O--CaO--P}_2\text{O}_5$ glass reinforced hydroxyapatite composite: a study by XPS analysis, J. Mater. Sci. Mater. Med. 7 (1996) 181.
- [6] G. Gabbi, A. Cacchioli, B. Locardi, E. Guadagnino, Bioactive glass coating: physicochemical aspects and biological findings, Biomaterials 16 (1995) 515.
- [7] H.A. Elbatal, M.A. Azooz, E.M.A. Khalil, A.S. Monem, Y.M. Hamdy, Characterization of some bioglass-ceramics, Mater. Chem. Phys. 80 (2003) 599.
- [8] K. Franks, I. Abrahams, G. Georgious, J.C. Knowles, Investigation of thermal parameters and crystallisation in a ternary $\text{P}_2\text{O}_5\text{--CaO--Na}_2\text{O}$ based glass system, Biomaterials 22 (2001) 497.
- [9] J.D. Santos, P.L. Silva, J.C. Knowles, S. Talal, F.J. Monteriro, Reinforcement of hydroxyapatite by adding $\text{P}_2\text{O}_5\text{--CaO}$ glasses with Na_2O , K_2O and MgO , J. Mater. Sci. Mater. Med. 7 (1996) 187.
- [10] R.M. Vallet-Regí, Static and dynamic in vitro study of a sol–gel glass bioactivity, Biomaterials 22 (2001) 2301.